Pergamon

Geochimica et Cosmochimica Acta, Vol. 68, No. 17, pp. 3557–3567, 2004

0016-7037/04 $30.00 + .00

doi:10.1016/j.gca.2003.12.012

Experimental determination of the activity-composition relations and phase equilibria of H_2O-CO_2-NaCl fluids at 500°C, 500 bars

L. M. Anovitz,[1,2,*] T. C. Labotka,[1] J. G. Blencoe,[2] and J. Horita[2]

[1]Department of Earth and Planetary Sciences, University of Tennessee, Knoxville, TN 37996, USA
[2]M.S. 6110, Bldg. 4500-S, Oak Ridge National Laboratory, Oak Ridge, TN 37831-6110, USA

(*Received November* 22, 2002; *accepted in revised form December* 3, 2003)

Abstract—An understanding of the activity-composition (*a–X*) relations and phase equilibria of halite-bearing, mixed-species supercritical fluids is critically important in many geological and industrial applications. We have performed experiments on H_2O-CO_2-NaCl fluids at 500°C, 500 bar, to obtain accurate and precise data on their *a–X* relations and phase equilibria. Two kinds of experiments were performed. First, H_2O-CO_2-NaCl samples were reacted at fixed activities of H_2O = 0.078, 0.350, 0.425, 0.448, 0.553, 0.560, 0.606, 0.678, 0.798, 0.841, and 0.935 to define the tie lines of known H_2O activity in the halite-vapor and vapor-brine fields. Results indicate that fluids with all but the last of these H_2O activities lie in the vapor-halite two-phase region and that a fluid with a_{H_2O} = 0.841 has a composition close to the three-phase (vapor + brine + halite) field. A second set of experiments was performed to determine the solubility of NaCl in parts of the system in equilibrium with halite. Data from these experiments suggest that the vapor corner of the three-phase field lies at H_2O contents above X_{H_2O} = 0.58 and X_{NaCl} = 0.06, and below X_{H_2O} = 0.75 and X_{NaCl} = 0.06, which is a significantly more H_2O-rich composition than indicated by existing thermodynamic models.

1. INTRODUCTION

Thermophysical data and equations of state for fluids have numerous applications in science and technology. Problems as varied as analysis of magma-hydrothermal systems and ore deposits, flow through pipes, metamorphic phase equilibria, treatment of toxic waste, and analysis of fluid inclusions require data on the thermodynamics, physical properties, and phase equilibria of pure and mixed fluids. Thus, it is unfortunate that the equations of state available for mixed fluids are often either wholly theoretical or based on sparse or imprecise experimental data.

H_2O, CO_2, and NaCl are the predominant fluid components in many geological systems. Although several thermodynamic models of the H_2O-CO_2-NaCl system have been proposed (Bowers and Helgeson 1983; Duan et al., 1995), relevant experimental data are scarce. In this paper we describe the results of a series of experiments performed at 500°C, 500 bar, to define the activity-composition (*a–X*) and phase relations of H_2O-CO_2-NaCl fluids. Our work on the H_2O-CO_2 system at 500°C, 500 bar (Anovitz et al., 1998) provides a well-determined dataset for one of the bounding binaries of this system. We extend that work by directly measuring the activity-composition and phase relations of H_2O-CO_2-NaCl fluids at 500°C and 500 bar. This pressure and temperature are highly significant in geochemistry and petrology because many contact-metamorphic, magma-hydrothermal, and ore-forming systems form at or near this pressure and temperature.

Data on H_2O-CO_2-NaCl fluids at 500°C, 500 bar are also important in the study of amphibolites and granulites because the excess Gibbs free energy and, therefore, the activity-composition relations of the system depend on the integral of the excess volume (V^{ex}) from 1 bar to the pressure of interest. As shown by Seitz and Blencoe (1999) for the H_2O-CO_2 system, the maximum excess volume falls at or near the pressure of the critical isochore. This has been observed for numerous mixed-volatile systems at all temperatures for which reliable volumetric data are available. While the values of V^{ex} are less well-known for strong electrolyte solutions, the data of Aranovich and Newton (1996) suggest that negative deviations from ideality in the H_2O-NaCl system increase most strongly from 2000 to 4200 bar and change relatively little to 15 kbar. The isothermal pressure dependence of the activity–composition relationships of a fluid system is obtained by integrating the excess volume from the pressure at which those relations are known to the pressure of interest (Blencoe et al., 1999). However, V_{ex} decreases rapidly above the pressure of the critical isochore, and thus the activity–composition relations of mixed fluids depend only weakly on pressure at higher pressures. Derivation of a thermodynamic model for mixing properties at all geologically relevant pressures depends critically on data obtained at low pressures, where the excess volumes are relatively large. Typically, this means pressures up to ~1000 bar above that of the critical isochore.

2. PREVIOUS WORK

While the experiments reported in the present paper provide highly accurate and precise measurements of H_2O-CO_2-NaCl activity-composition and phase relations at 500°C, 500 bar, the interpretation of our results depends strongly on available data for the limiting binaries, which were used both to help plan our experiments and to interpret our data. Because of its wide-ranging geological and industrial significance, there have been numerous studies of the thermodynamics and phase relations of parts of the H_2O-CO_2-NaCl ternary, but in most of those investigations attention was primarily focused on H_2O-rich

* Author to whom correspondence should be addressed (lanovitz@utk.edu).

compositions at lower pressures and temperatures. The *P-T-X* range of the available data is limited. The results of those studies are summarized below, exclusive of low-temperature studies well outside of the temperature range of interest here.

The H_2O-NaCl system. The thermodynamics and phase equilibria of the H_2O-NaCl join have been studied extensively. Early investigations include the work of Keevil (1942), Ölander and Liander (1950), Copeland et al. (1953) and Morey (1957). Sourirajan and Kennedy (1962) performed experiments at temperatures up to 700°C, but some of their results are inconsistent with those of more recent investigators. Data obtained from experiments performed at 300 to 500°C were summarized by Bischoff and Pitzer (1989) and Bischoff (1991). More recent studies have been conducted by Knight and Bodnar (1989), who studied the critical curve from 0 to 30% NaCl up to 820°C and 1574 bar, Bodnar (1994), who determined the halite liquidus and isochores for 40 wt.% NaCl fluid at 350–800°C and 1000–6000 bar, and Aranovich and Newton (1996), who conducted experiments from 600 to 900°C and 2000 to 15000 bar.

There have been nearly as many models proposed for the H_2O-NaCl system as experiments conducted on it. As discussed by Anderko and Pitzer (1993), who presented a comprehensive equation of state for the system from 573 to 1200 K up to 5000 bar, the excess Gibbs energy model of Pitzer (1984) successfully represents the available data below 573 K. The models of Pitzer and Simonson (1986) and Pabalan and Pitzer (1990) extended the Pitzer approach to 623 K. Pitzer and Pabalan (1986) modeled the properties of the vapor phase at higher temperatures up to the pressure of the three-phase assemblage using a successive hydration model. Tanger and Pitzer (1989) and Levelt-Sengers and Gallagher (1990) developed models that reproduce the compositions of the vapor-liquid two-phase region from 573 to 873 K. None of these equations, however, correctly predicts the behavior of H_2O-NaCl fluids with liquid-like densities. Those densities, but not the phase relations or chemical potentials, were modeled by Lvov and Wood (1990). Knight and Bodnar (1989) provided expressions for the pressure, temperature, and specific volume of the critical point, and Sterner et al. (1992) devised a single-parameter Margules model to represent the liquidus surface.

Together with the data summaries of Bischoff and Pitzer (1989) and Bischoff (1991) the studies discussed above provide a reasonably clear picture of phase relations for the H_2O-NaCl binary and, for present purposes, the phase relations expected for the H_2O-NaCl boundary of the H_2O-CO_2-NaCl system at 500°C, 500 bar. Progressing from H_2O-rich to NaCl-rich compositions, the phase diagram consists of a one-phase vapor field, a two-phase vapor plus brine field, a one-phase brine field, a two-phase brine plus halite field, and finally single-phase halite. The H_2O-rich vapor contains a maximum of 0.42 mol % NaCl, whereas high-density brine contains a minimum of 14.8 mol % NaCl and a maximum of 33 mol % NaCl. Halite is assumed to be pure NaCl.

The H_2O-CO_2 system. The critical curve for the H_2O-CO_2 system originates at the critical point of pure H_2O (374.15°C, 221.2 bar). With increasing pressure the temperature of the critical curve first drops to a minimum near 266°C, 2250 bar, and $X_{H_2O} = 0.585$ (Tödheide and Franck, 1963) and then increases. Complete solution between H_2O and CO_2 is to be expected in our experiments because they were conducted at *P-T* conditions above this curve. The available activity-composition data for the H_2O-CO_2 system were summarized by Joyce and Blencoe (1994) and Anovitz et al. (1998), and the *a–X* relations of the H_2O-CO_2 binary at 500°C and 500 bar were determined by Anovitz et al. (1998). In the latter study, *a–X* data were acquired in essentially the same manner as described below for H_2O-CO_2-NaCl mixtures, and the results provide a well-defined limiting case for the ternary. Recently Aranovich and Newton (1999) studied the *a–X* relations in the H_2O-CO_2 system from 600 to 1000°C and 6–14 kbar. The data of both Anovitz et al. (1998) and Aranovich and Newton (1999) suggest that H_2O-CO_2 fluids exhibit positive deviations from ideal mixing in the *P-T* ranges studied.

The CO_2-NaCl system. Very few experimental data exist on mixing in the CO_2-NaCl binary. The only published results are those of Grjotheim et al. (1962), who studied this join from 810 to 950°C at 1 atm. At 850° and 950°C the solubility of CO_2 in molten NaCl is 4.6×10^{-6} and 6.0×10^{-6} mol CO_2/cm^3 NaCl, respectively. Thus, CO_2 has very low solubility in NaCl in this temperature range at 1 atm. No corresponding data are available on the solubility of NaCl in CO_2, but it is probably small. The effect of pressure is completely unknown.

The H_2O-CO_2-NaCl system. Although there have been several studies of the H_2O-CO_2-NaCl system, the ranges of pressure, temperature, and composition that have been explored are severely limited. In addition, the results from several of these studies are inconsistent (e.g., Kotel'nikov and Kotel'nikova 1991 vs. Bowers and Helgeson 1983 at 2000 bar). Previous studies of the H_2O-CO_2-NaCl system are summarized in Table 1, examination of which reveals several important points. First, the data coverage is spotty (more so when the individual experiments within the ranges quoted for each study are considered), especially for temperatures above 500°C and pressures below 4000 bar. This is a critically important *P-T* range because, as noted above, excess volumes of mixing are greatest at low pressures and because activity-composition models for high pressures strongly depend on the lower pressure values (cf. Seitz and Blencoe 1999; Blencoe et al., 1999). The available data, even from the more comprehensive studies (e.g., Schmidt 1997 and Shmulovich and Graham 1999), primarily delineate the boundaries of the liquid-vapor two-phase field. Very few data are available on the orientations of tie lines, the location of the three-phase field, or activity-composition relations, particularly for NaCl- and CO_2-rich compositions.

3. EXPERIMENTAL TECHNIQUES

Two kinds of experiments were performed. In the first, an improved version of the fixed-H_2O activity technique was used to locate isoactivity tie-lines within the H_2O-CO_2-NaCl ternary (Joyce and Holloway 1993; Joyce and Blencoe 1994; Anovitz et al., 1998). This approach has the advantage that the property of greatest interest, the relationship between activity and composition, is measured directly and is not derived from other data. The second kind of experiment measured the solubility of NaCl to place limits on the locations of the phase boundaries in the system.

Figure 1 schematically illustrates the phase relations of the H_2O-CO_2-NaCl system at 500°C and 500 bar and the experimental techniques used to determine the *a–X* relations. The phase diagram contains three one-phase fields defining the stability limits of an H_2O-CO_2-rich vapor, an H_2O-NaCl-rich brine, and halite. There are also the two-phase fields halite + vapor, halite + brine, and vapor + brine and the three-phase field halite + vapor + brine.

Table 1. Experimental and theoretical studies of the H_2O-CO_2-NaCl system, excluding clathrates.

Reference	Pressure (kb)	Temp (°C)	Compositional range	Comments
Anovitz et al. (this study)	0.5	500–800	ternary	Fixed activity and phase-equilibrium experiments
Bowers and Helgeson (1983)	0–2	400–600	H_2O-CO_2-$X_{NaCl} < 0.3$	model
Brown and Lamb (1989)	2–10	>350	<6 wt% NaCl	Calculation of isochores
Darimont (1987)				Data comparison
Drummond (1981)	<0.378	25–400	0–6 m NaCl	Experiments: CO_2 in H_2O-NaCl solutions
Duan et al. (1995)	0–6	300–1000	<30 wt% NaCl	Vapor-liquid model, does not predict saturation surface
Ellis and Golding (1963)	<0.0919	<330	0–2 m NaCl	Experiments: CO_2 in H_2O-NaCl solutions
Franz et al. (1992)	1–3	500–700	$X_{NaCl} < 0.2$ $X_{CO_2} < 0.5$	Experiments: no three-phase data, limits of NaCl solubility in fluid
Gehrig (1980)	< 3	25–560	6, 10, 20 wt% NaCl	Experiments: isopleths and two-phase regions
Hendel and Hollister (1981)	1–2	200–350	2.6 wt% NaCl	Natural samples
Jacobs and Kerrick (1981)	2,6	450–600	5, 10 wt% NaCl	Experiments: a/X data, effects of ternary compositions on decarbonation equilibria
Johnson (1991)	6.6–7.5	890–960	<50 wt% NaCl $0.1 < x_{CO_2} < 0.5$	Experiments: synthetic fluid inclusions, liquid-vapor miscibility
Johnson (1992)	6.0–7.6	870–960	6–23.9 wt% NaCl $0.1 < x_{CO_2} < 0.51$	Experiments: synthetic fluid inclusion PVT data
Joyce and Holloway (1993)	2	700–850	ternary	Experiments: four isoactivity curves
Kotel'nikov and Kotel'nikova (1991)	1–2	400–800	$X_{H_2O} > 0.5$	Experiments: synthetic fluid inclusions one- or two-phase fields, no tie lines or three-phase fields
Kotel'nikova and Kotel'nikov (1997)	5	700		Experiments: synthetic fluid inclusions
Malinin and Kurovskaya (1975)	0.05	25, 100, 150	0–6 m NaCl	Experiments: solubility of CO_2 in H_2O-NaCl solutions
Malinin and Savelyeva (1972)	0.05	25, 50, 75	0–4.5 m NaCl	Experiments: solubility of CO_2 in H_2O-NaCl solutions
Naumov et al. (1974)	0.6–2.5	100–500	0–5 Ionic strength	Model solubility of CO_2 in H_2O-NaCl solutions from natural samples and extrapolation of lower P-T experiments from the literature
Popp and Franz (1989)	1–3	500–700	0.5–4 m NaCl > 60 wt% H_2O	Experiments: synthetic fluid inclusions, 1 or 2-phase fields. No tie lines of three-phase fields
Plyusnina (1990)	1	200–300	$XCO_2 < 0.2$ 1 m NaCl	Experiments: a-X data, effects of ternary compositions on epidote equilibria
Schmidt (1997)	1–5	300–800	<40 wt% NaCl <20 wt% CO_2	Experiments: synthetic fluid inclusions, liquid-vapor boundaries, isohomogenization lines
Shmulovich and Graham (1996)	5–9	700–900	H_2O-NaCl-albite	Experiments: H_2O-NaCl-albite melting experiments
Shmulovich and Plyasunova (1993)	5	500	10–25% salinity	Experiments: synthetic fluid inclusions, liquid-vapor boundary
Sterner et al. (1984)	1	500	12, 20% NaCl	Experiments: liquid-vapor boundary
Takenouchi and Kennedy (1965)	0.1–1.4	150–450	6, 20% NaCl	Experiments: solubility of CO_2 in H_2O-NaCl fluids
Yasunishi and Yoshida (1979)	0.001	15–35	0.5–5 M NaCl	Experiments: CO_2 solubility in H_2O-NaCl fluids

Experiments were conducted in a hydrogen-service, internally heated gas apparatus with a large internal volume, which permits simultaneous reaction of several encapsulated samples that, in turn, provide isoactivity reversal brackets at fixed P and T. Temperature was monitored with three thermocouples placed at the bottom, in the middle, and at the top of the sample holder. Temperature was controlled using a dual-channel Micristar controller and a two-zone, kanthal-wound furnace, the upper and lower windings of which were controlled by the upper and lower thermocouples to minimize thermal gradients. Temperature readings among the three thermocouples typically varied by approximately 1°C, suggesting that the overall thermal gradient in the sample holder was less than ± 5°C. Pressure was measured using a calibrated 60000 psig pressure transducer. Experiments were run for at least 1 week, and several ran for as long as 4 weeks.

In the fixed-H_2O-activity method the activity of H_2O is set by fixing oxygen fugacity (f_{O_2}) with a metal—metal-oxide buffer and by fixing hydrogen fugacity (f_{H_2}) with an Ar-H_2 pressure medium. During the experiment, the hydrogen fugacity is monitored with a Shaw membrane (Shaw 1963, 1967). In the experiments presented here Ni-NiO was used as the metal—metal-oxide oxygen buffer, and the f_{O_2} value defined experimentally by Anovitz et al. (1998) was used to calculate a_{H_2O}. Together, the known f_{O_2} and f_{H_2} values fix H_2O activity through

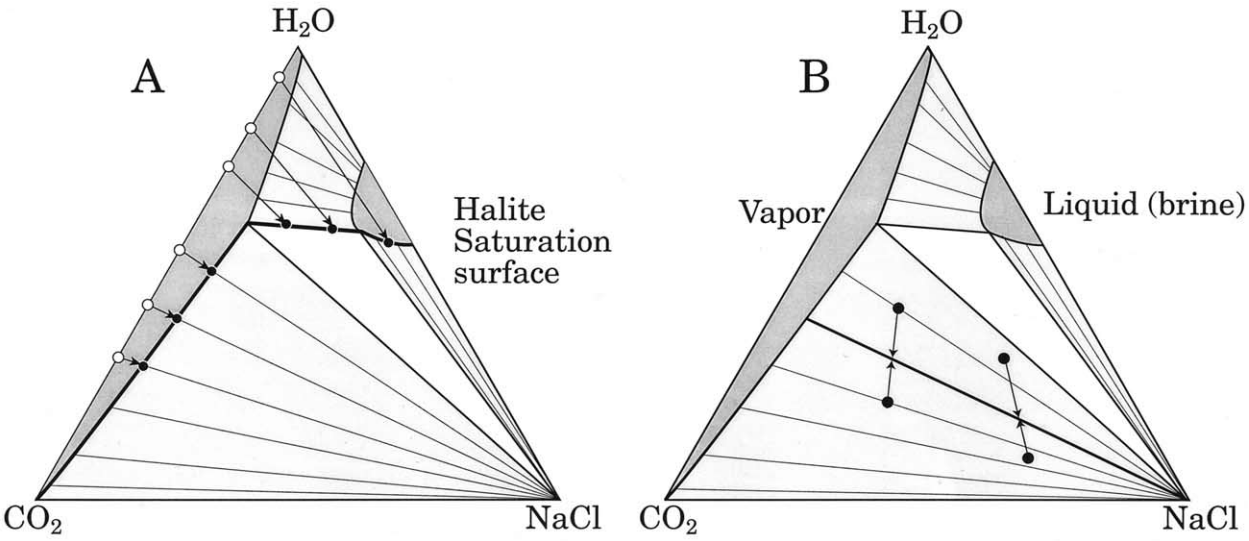

Fig. 1. Schematic illustration of the phase equilibria in the H_2O-CO_2-NaCl system and the experimental approaches used to determine *a–X* relations and phase equilibria in this study. Figure A shows the NaCl-saturated phase equilibrium experiments, and figure B shows the fixed-H_2O activity experiments.

the equilibrium $H_2O = H_2 + 1/2\ O_2$. The equilibrium mole fraction of H_2O corresponding to that H_2O activity is then experimentally reversed (approached from opposite compositional directions to bracket the equilibrium value without assuming equilibrium has been achieved) by measuring the changes in the H_2O contents of samples whose initial compositions were either more or less H_2O-rich than the equilibrium value.

In the *a–X* experiments, 5 cm long × 5 mm o.d. $Ag_{25}Pd_{75}$ capsules were loaded with water, silver oxalate as a source for CO_2, NaCl, and Ni + NiO to buffer f_{O_2}. The amount of water initially added to each run is listed in Table 2, and excess amounts of NaCl, Ni, and NiO were used. The NaCl was placed in a small (1cm × 3 mm) Pt inner capsule with only the lower end welded shut, which was placed in the outer capsule assembly last. To fix the H_2O activity, the fugacity of hydrogen was selected by using an H_2—Ar pressure medium of known composition. In general, the fugacity of hydrogen equals the mole fraction of hydrogen in the pressure medium multiplied by the total pressure. Although the hydrogen content of the gas and the pressure and temperature of the run fix the nominal hydrogen fugacity, some hydrogen is absorbed by the pressure vessel and may be released during a subsequent experiment. Thus, the actual hydrogen fugacity during an experiment varies from the nominal value. The hydrogen fugacity for each experiment is, therefore, measured using a $Ag_{25}Pd_{75}$ Shaw membrane placed next to the capsules and connected by capillary tubing (to minimize volume) to a calibrated, high-precision 20 psia pressure transducer (see Anovitz et al., 1998 for additional details). The membrane was supported internally with alumina powder and was evacuated to <0.01 bar before each experiment. Because $Ag_{25}Pd_{75}$ is highly permeable to hydrogen but not to argon (Rubin 1966; Ackerman and Koskinas 1972, Holleck 1970, Huebner 1971, Chou 1987, Gunter et al., 1987), the pressure inside the membrane equals the fugacity of hydrogen in the much higher-pressure gas in the pressure vessel.

Figure 1 illustrates the method used to determine and, where possible, reverse, the positions of tie-lines and phase boundaries. Each experiment contained eight to twelve capsules. For the isoactivity experiments, starting compositions were chosen so that each contains either more or less H_2O than the expected equilibrium value. The sample compositions cover a range of CO_2/NaCl ratios and expected changes in the mole fraction of H_2O. In capsules that initially contained more H_2O than was stable for a given H_2O activity, the H_2O reacted with Ni metal to form NiO and H_2; the H_2 then diffused through the $Ag_{25}Pd_{75}$ capsule into the pressure medium. In capsules that initially contained less than the equilibrium mass of H_2O, H_2 from the pressure medium diffused into the capsule and reacted with NiO to form Ni and H_2O. Such paired reactions provide reversals of equilibrium H_2O contents at known H_2O activities.

The solubility of halite in vapor or vapor + brine mixtures along the boundary of the three-phase field was determined by measuring the loss of halite from the inner capsules. We conducted additional solubility experiments without Ni and NiO. In those experiments the outer capsules were platinum, no Ni-NiO was added, and the pressure medium was Ar because there was no need to control a_{H_2O}. The volume of the inner capsule is small relative to that of the outer capsule, and the NaCl dissolved during the experiment precipitated primarily outside the inner capsule during the quench. Thus, the amount of NaCl remaining in the inner capsule after the experiment provides a measure of the amount dissolved in the known amount of fluid. This constitutes a half-reversal on the location of the halite saturation surface.

4. ANALYTICAL TECHNIQUES

In our previous work using the fixed H_2O-activity technique (Anovitz et al., 1998) we developed new vacuum-line manometric techniques for precise and accurate measurement of the H_2O and gas contents of reacted samples to obtain more reliable *a–X* data for the H_2O-CO_2 and H_2O-N_2 systems. While analysis of ternary H_2O-CO_2-NaCl samples required some modifications of these procedures, the overall approach is very similar.

To analyze a sample, the outer capsule was first punctured in a vacuum line using a custom puncturing device, then warmed with a heat gun to expel all the H_2O and CO_2 gas, which were separated cryogenically. The H_2O was then reacted with uranium at 800°C (Bigeleisen et al., 1952). The resulting H_2 was pumped into a standard volume with a Toepler pump, and the pressure in that volume was measured by a mercury manometer. CO_2 was transferred cryogenically into a separate reference volume, and its pressure was measured by a pressure transducer. Typically the yield of CO_2 from our synthetic silver oxalate was 98–100%; the analyzed amount of CO_2 was used in all subsequent calculations. The precision of this technique was discussed by Anovitz et al. (1998). As in that study, if the measured change in the amount of H_2O in the capsule was <2 μmoles, the result was not considered a reliable indication of reaction direction.

Analysis of the NaCl contents in the fluid was more straightforward. In each sample halite was initially loaded into the inner capsule. After the experiment and manometric analysis of the fluid, the outer capsule was opened, and the inner capsule extracted and cleaned to remove loosely adhering Ni, NiO, Ag, and NaCl. The inner capsule was then weighed and cut in half lengthwise. The halves were twisted to open the

Table 2. Data for H_2O-CO_2-NaCl fixed-activity experiments at 500°C, 500 bar.

Capsule	ppm H_2	P_{H_2} (bar)	a_{H_2O}	Initial X_{H_2O}	Initial X_{NaCl}	Final X_{H_2O}	Final X_{NaCl}	Δ μmoles H_2O
5-7-98-1	1790	13.49	0.7976	0.6520	0.1754	0.6403	0.1813	−12.40
5-7-98-2	1790	13.49	0.7976	0.7346	0.1090	0.7203	0.1149	−20.76
5-7-98-3	1790	13.49	0.7976	0.7162	0.0587	0.7090	0.0602	−10.67
5-7-98-4	1790	13.49	0.7976	0.6891	0.0805	0.6915	0.0799	2.36
5-7-98-7	1790	13.49	0.7976	0.0000	0.7665	0.0934	0.6949	50.82
5-7-98-8	1790	13.49	0.7976	0.0000	0.7103	0.2267	0.5496	18.57
5-21-98-9	1500	10.25	0.6060	0.5173	0.0485	0.5025	0.0500	−10.25
5-21-98-10	1500	10.25	0.6060	0.4672	0.1351	0.4739	0.1335	4.18
5-21-98-11	1500	10.25	0.6060	0.4237	0.2261	0.4092	0.2295	−8.20
5-21-98-15	1500	10.25	0.6060	0.0000	0.6972	0.1231	0.6114	21.60
5-21-98-16	1500	10.25	0.6060	0.0000	0.7494	0.0968	0.6769	30.44
6-6-98-19	1274	7.19	0.4251	0.3394	0.0579	0.3574	0.0563	15.87
6-6-98-20	1274	7.19	0.4251	0.4159	0.0622	0.4234	0.0614	7.99
6-6-98-21	1274	7.19	0.4251	0.2855	0.0733	0.3058	0.0712	13.96
6-22-98-26	1790	11.47	0.6782	0.4966	0.1031	0.5213	0.0963	6.74
6-22-98-30	1790	11.47	0.6782	0.5099	0.1551	0.5168	0.1529	3.59
6-22-98-33	1790	11.47	0.6782	0.5580	0.2239	0.5312	0.2375	−13.22
6-22-98-34	1790	11.47	0.6782	0.6171	0.1818	0.5972	0.1912	−4.99
6-22-98-35	1790	11.47	0.6782	0.5484	0.1364	0.5443	0.1377	−7.01
12-8-95-7	1280	9.47	0.5599	0.0000	0.5246	0.2602	0.3882	207.23
12-8-95-8	1280	9.47	0.5599	0.4100	0.3127	0.3753	0.3311	−28.31
7-13-98-39	1274	7.57	0.4476	0.4321	0.1170	0.4329	0.1168	0.48
7-13-98-41	1274	7.57	0.4476	0.5494	0.0518	0.4960	0.0579	−16.80
7-13-98-43	1274	7.57	0.4476	0.3410	0.0571	0.3674	0.0548	17.97
NCH 54	2000	14.22	0.8408	0.7598	0.0717	0.7564	0.0727	−1.64
NCH 57	2000	14.22	0.8408	0.8145	0.1211	0.8065	0.1263	−7.11
NCH 58	2000	14.22	0.8408	0.7517	0.1733	0.7471	0.1765	−3.00
NCH 61	2000	14.22	0.8408	0.6390	0.3371	0.3530	0.6040	−37.24
NCH 62	2000	14.22	0.8408	0.7588	0.2224	0.1364	0.7962	−64.32
8-12-98-63	2000	14.22	0.8408	0.8450	0.1190	0.6236	0.2891	−40.57
NCH 65	1000	5.92	0.3500	0.1774	0.4015	0.1826	0.3989	1.52
NCH 66	1000	5.92	0.3500	0.1260	0.4600	0.1931	0.4247	16.49
NCH 67	1000	5.92	0.3500	0.2878	0.3470	0.2764	0.3526	−2.75
NCH 69	1000	5.92	0.3500	0.1741	0.2058	0.2006	0.1992	3.80
NCH 71	1000	5.92	0.3500	0.1861	0.5658	0.1756	0.5732	−1.91
NHC87	758	1.32	0.0780	0.1152	0.2281	0.0463	0.2458	−24.71
NHC90	758	1.32	0.0780	0.0591	0.6245	0.0362	0.6397	−13.86
NHC91	758	1.32	0.0780	0.0781	0.6021	0.0196	0.6403	−19.50
NHC93	1500	9.36	0.5534	0.4339	0.1451	0.4222	0.1480	−2.08
NHC94	1500	9.36	0.5534	0.4366	0.1424	0.4414	0.1412	0.94
NHC95	1500	9.36	0.5534	0.4872	0.1269	0.4913	0.1259	1.47
NHC96	1500	9.36	0.5534	0.5068	0.1200	0.4919	0.1236	−3.60
NHC98	1500	9.36	0.5534	0.2785	0.4048	0.3407	0.3699	11.29
NHC99	1500	9.36	0.5534	0.3525	0.3307	0.3875	0.3128	6.12
NHC102	1500	9.36	0.5534	0.3843	0.3000	0.3810	0.3016	−0.94
NHC103	1500	9.36	0.5534	0.4500	0.2801	0.4415	0.2844	−2.00
NHC109	2250	15.82	0.9354	0.7396	0.2239	0.7414	0.2223	8.32
NHC113	2250	15.82	0.9354	0.7842	0.0791	0.7744	0.0827	−4.87
NHC114	2250	15.82	0.9354	0.7874	0.1826	0.7881	0.1820	1.16
NHC117	2250	15.82	0.9354	0.8251	0.0605	0.8285	0.0594	5.78
NHC119	2250	15.82	0.9354	0.8169	0.0802	0.7979	0.0885	−8.61
NHC120	2250	15.82	0.9354	0.8380	0.1338	0.8350	0.1363	−3.67

capsule, and the two parts were placed in water and heated in an ultrasonic cleaner to dissolve the NaCl. After dissolution the capsule halves were dried and reweighed. The change in weight yielded the mass of NaCl remaining in the inner capsule. The difference between this and the initial weight of halite in the inner capsule yielded the amount of NaCl dissolved in the fluid during the experiment. With the exception of NaCl, only loosely adhering particles that might fall off during the remainder of the analysis had to be removed during the cleaning operation, because firmly attached particles would not affect the results. All weighings were performed with the same Mettler A163 analytical balance, having a precision of 0.01 mg. The balance was calibrated before each weighing session.

In our experience with this technique, the initial drying step is critical to the quality of the result. The capsules used for the fixed H_2O-activity experiments were dried very thoroughly as part of the fluid analysis. Use of a high-vacuum line, a heat gun, and a liquid-nitrogen trap efficiently removed water from the remaining salt. For the experiments with the platinum outer capsules, the inner capsules were dried in a vacuum oven after removal from the outer capsule.

5. RESULTS

The results of our activity–composition and phase equilibrium experiments are shown in Figures 2 and 3 and listed in Tables 2 and 3. The tables show the change in the number of micromoles of H_2O observed for each sample, as well as the initial and final mole fractions of H_2O in the fluid.

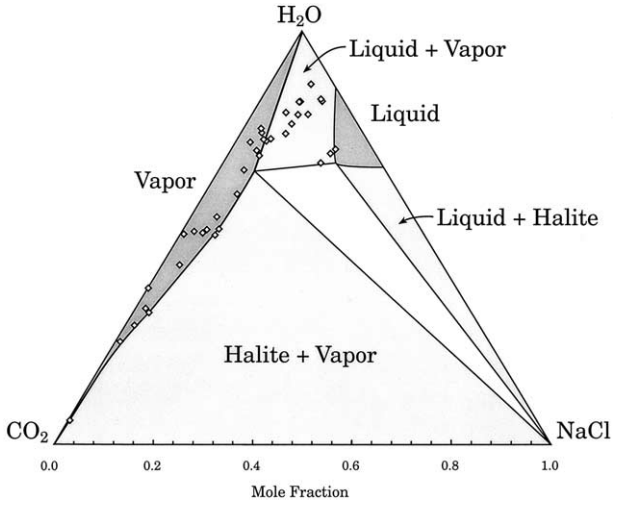

Fig. 2. Results obtained from experiments performed to locate the phase equilibrium boundaries in the H_2O-CO_2-NaCl system at 500°C, 500 bar. Because data were only obtained on the H_2O-CO_2-NaCl vapor saturation surface and the vapor-brine edge of the three phase field, other ternary phase boundaries are only constrained at their binary endpoints or where they intersect the experimentally determined curves, and their positions should be considered tentative or schematic.

5.1. Phase Boundary Results

Figure 2 shows the data that locate the phase boundaries in the H_2O-CO_2-NaCl system at 500°C, 500 bar. The starting fluid compositions are assumed to lie on the H_2O-CO_2 binary at the location dictated by the amounts of H_2O and silver oxalate loaded into the capsules. The generation of CO_2 from the Ag oxalate and its subsequent mixing with water is assumed to occur before NaCl dissolution because halite was originally held in the inner capsule. The change in fluid composition during the experiment may have been more complex, but the final composition still provides a half reversal of the equilibrium boundary.

The diamonds shown in Figure 2 represent final fluid compositions. Because some samples failed to reach equilibrium and because reversals with NaCl-supersaturated solutions were impossible, the maximum solubility results were used to locate the NaCl saturation surface. The data limit both the maximum amount of NaCl soluble in an H_2O-CO_2 fluid and the position of the vapor-brine edge of the three-phase field. The vapor-brine tie line was determined from solubility experiments in which the bulk composition of the system lay within the three-phase field. The analytical techniques used cannot distinguish high-pressure, high-temperature brine from vapor compositions because the vapor and brine are combined by the quench and analysis. Thus, the endpoints of this tie line cannot be determined directly. Nonetheless, the location can be, and it is possible to locate the ends from inflection points in the solubility curve. For instance, the vapor end point can be determined from the intersection of the vapor-brine tie line with the vapor-saturation curve, which, as can be seen from Figure 2, generally meet at a high angle.

The phase equilibrium results shown in Figure 2 suggest, first, that in the vapor + halite field the solubility of NaCl in the vapor does not appear to be a linear function of H_2O/CO_2 ratio. Instead, it appears to be low up to a mole fraction of H_2O close to 0.30; in more water-rich vapor the solubility increases rapidly to ~7.5 mol %. Thermodynamic modeling suggests that this is reasonable. Figure 2 also shows that there is some inconsistency in the data used to locate the vapor-brine edge of the three-phase field. Above X_{H_2O} of ~0.66 the data suggest two possible locations for the saturation curve. Most of the data suggest a vapor boundary without a noticeable inflection. Three samples, however, suggest a much higher NaCl content and imply that the H_2O content of the vapor corner of the three-phase field was exceeded in the other samples. Later work suggests an explanation for this anomalous result. In most experiments, the crimped end of the inner capsule was on top. Transport of NaCl from the inner to the outer capsule under these conditions can only occur in the vapor phase. Under conditions where a brine phase is stable, some brine may precipitate in the outer capsule, but most remains in the inner capsule on the halite. On quenching, the NaCl in this brine remains in the inner capsule, and the results, therefore, significantly underestimate the NaCl content of the vapor-brine edge of the three-phase field. In our later experiments (Anovitz et al., 2002) this problem was addressed by orienting the inner capsule with the crimped end down, after first melting the NaCl in it to prevent grains from falling out while the capsule is inverted. Therefore, we believe that the samples having higher halite solubility more accurately indicate the location of the vapor-brine edge of the three-phase field.

5.2. Activity-Composition Results

Figure 3 shows the results of the fixed H_2O-activity experiments. The circles represent starting fluid compositions, and the triangles indicate final values. For each sample, the only possible change in the composition is a change in H_2O content. Thus the initial and final fluid compositions fall on a line that intersects the H_2O corner of the phase diagram. The positions of the isoactivity curves (curves of constant a_{H_2O}) and tie lines are fixed by the data for the H_2O-CO_2 system at $X_{NaCl} = 0$ and by our new experimental data in the middle. In addition, tie lines in the vapor + halite field end at pure NaCl. In general, the isoactivity curves in the vapor field are not collinear with the two-phase tie lines. As can be seen, in many cases tight reversals of the positions of the isoactivity lines were obtained.

Despite the regularity of the data, some inconsistencies exist. For the experiment performed at $a_{H_2O} = 0.798$ the mole fraction of H_2O in sample 5-7-98-4 increased from 0.6891 to 0.6915 with a change in H_2O content of 2.36 μmoles. This result is inconsistent with the results from sample NCH 62, which limits the location of the $a_{H_2O} = 0.841$ tie line to less H_2O-rich conditions. This total change in H_2O in sample 5-7-98-4 is small, however, and that for NCH 62 is relatively large (64.32 μmoles). Thus, the results for sample 5-7-98-4 could reflect analytical error.

The largest apparent inconsistency, however, is for the experiment conducted at $a_{H_2O} = 0.606$. Two samples reacted in this experiment, 5-21-98-15 and 5-21-98-16, initially contained no H_2O and yielded final H_2O contents that do not provide strong constraints on the location of the tie line. The measured H_2O contents of the other three samples reacted in that exper-

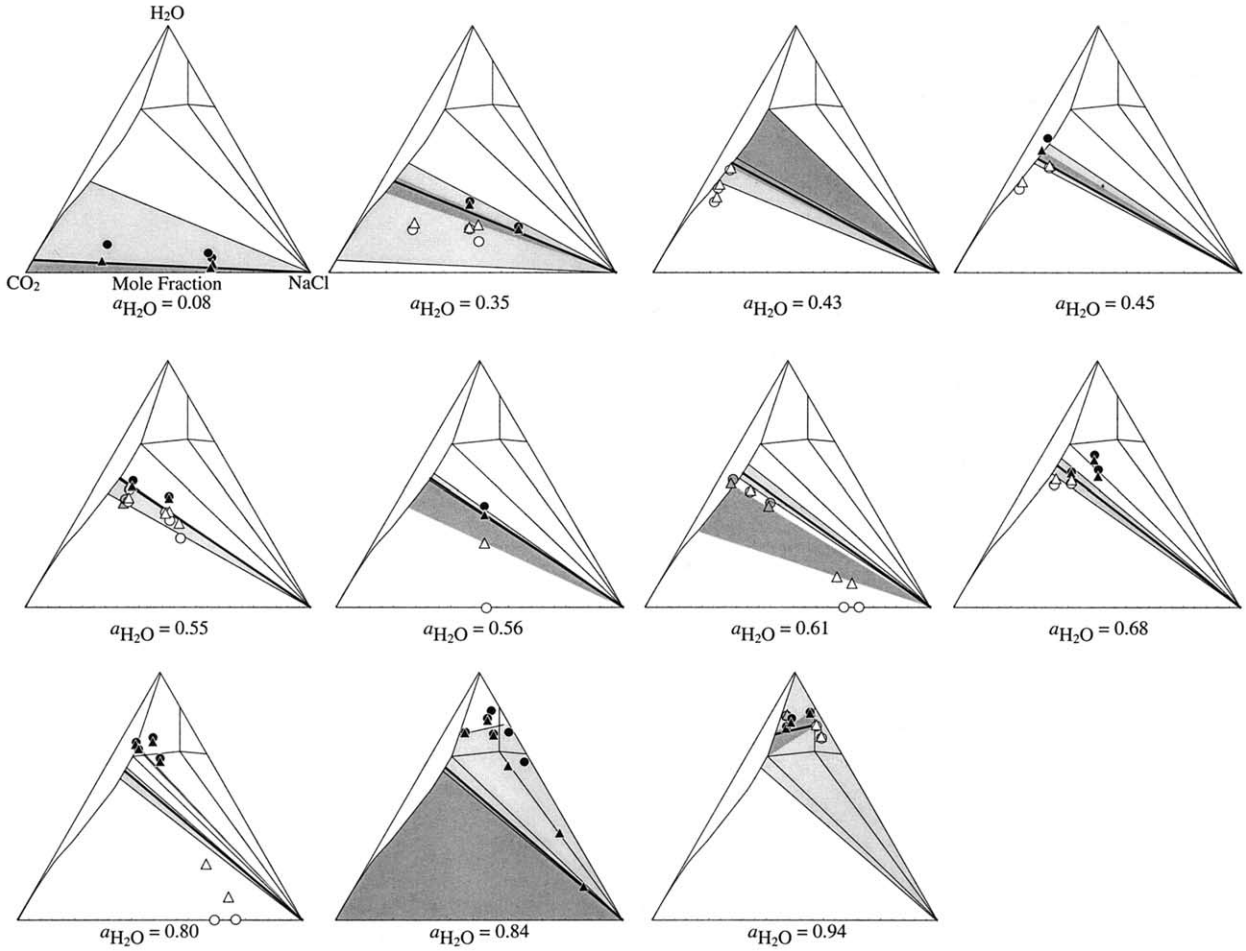

Fig. 3. Results obtained from fixed-activity experiments. Circles represent starting fluid compositions, and triangles represent final values. Open symbols show an H_2O-increase, and filled symbols show an H_2O decrease. Gray circle–triangle pairs are inconsistent with the results from the remaining experiments at a given activity. The dark gray region is the range of possible locations for a given fixed-activity tie line, as constrained by the experiments at that activity, and the heavy line is the selected location for that tie line. The light lines and the light gray regions show possible locations for the tie line constrained by the experiments at higher and lower activities.

iment, 5-21-98-9, 5-21-98-10 and 5-21-98-11, are mutually inconsistent. Both 5-21-98-9 and 5-21-98-11 indicate H_2O contents that are too low in comparison with values obtained from the experiment performed at $a_{H_2O} = 0.553$. Because 5-21-09-9 is actually in the one-phase vapor field, its anomalous H_2O content may reflect curvature in the isoactivity line in that field, although there is no independent evidence of this. The measured H_2O content of sample 5-21-98-11, however, remains inconsistent and is considered to be an outlier.

With the exception of the data points just discussed, the phase diagram for the H_2O-CO_2-NaCl system at 500°C and 500 bar, shown in Figure 3, has been drawn in a manner consistent with all the experimental data obtained. A combination of the phase equilibrium and fixed-H_2O-activity experiments was used to determine the location of the vapor corner of the three-phase field. The upper limit is set by the experiment performed at $a_{H_2O} = 0.94$, which was determined to lie in the vapor-brine field. While the position of this point cannot be determined accurately using our approach, it is approximately $X_{H_2O} = 0.75$, $X_{NaCl} = 0.06$.

The minimum H_2O content of the vapor corner of the three-phase field is less well determined. It certainly lies above the tie line for $a_{H_2O} = 0.68$, and therefore above $X_{H_2O} = 0.58$. The choice of a more limiting value depends on the uncertainties assigned to the two samples 5-7-98-4 and NCH 62, which were reacted at $a_{H_2O} = 0.80$ and $a_{H_2O} = 0.84$. If, as suggested above, the value for sample NCH 62 is correct and for sample 5-7-98-4 is erroneous, then the vapor end of the $a_{H_2O} = 0.84$ tie line must lie below $X_{H_2O} = 0.63$. Because only a maximum-H_2O half-reversal was obtained in this experiment, the location of the vapor corner of the three-phase field is not fixed. The most constraining experimental datum remains that for the $a_{H_2O} = 0.68$ experiment. On the other hand, if the value of X_{H_2O} obtained from sample 5-7-98-4 is correct and that for sample NCH 62 is not, the vapor corner must lie at $X_{H_2O} \geq 0.71$. This is considered unlikely because of the large difference in the change in H_2O content between the two samples. The location of the vapor corner of the three-phase field shown in Figures 2, 3, and 4 is the average of the limiting values: $X_{H_2O} = 0.665$.

Table 3. Data for H_2O-CO_2-NaCl salt-saturated vapor experiments at 500°C, 500 bar.

Capsule	Initial X_{H_2O}	Initial X_{NaCl}	Final X_{H_2O}	Final X_{NaCl}	Δ μmoles NaCl
NCH 11	0.5475	0	0.5110	0.0450	76.14
NCH 1	0.7907	0	0.7330	0.0628	20.19
NHC 3	0.7609	0	0.7300	0.0320	11.98
NHC 4	0.7495	0	0.7105	0.0547	16.08
NHC 9	0.5437	0	0.5151	0.0262	8.56
NHC 10	0.5402	0	0.5193	0.0499	15.91
6-6-98-19	0.3602	0	0.3775	0.0031	1.369
6-6-98-20	0.4435	0	0.4343	0.0371	25.59
6-6-98-21	0.3080	0	0.3182	0.0334	15.74
NHC 65	0.2964	0	0.2874	0.0198	2.91
NHC 66	0.2333	0	0.3284	0.0217	2.74
NHC 69	0.2192	0	0.2478	0.0107	1.03
NHC 72	0.9507	0	0.8698	0.0851	269.66
NHC 73	0.9042	0	0.8281	0.0842	173.50
NHC 74	0.8801	0	0.7965	0.0950	240.75
NHC 75	0.8604	0	0.8016	0.0684	144.07
NHC 78	0.7799	0	0.7364	0.0558	89.66
NHC 76	0.8281	0	0.7507	0.0934	180.52
NHC 80-1	0.8775	0	0.7032	0.2070	715.40
NHC 81-1	0.7875	0	0.7527	0.0441	65.53
NHC 82-1	0.9056	0	0.7134	0.2125	736.10
NHC 82-2	0.5128	0	0.5083	0.0088	12.32
NHC91	0.1963	0	0.0541	0.0092	1.03
NHC 95	0.5580	0	0.5207	0.0735	12.83
NHC 102	0.5461	0	0.5059	0.0726	9.58
NHC 125	0.9502	0	0.8282	0.1283	132.44
NHC 126	0.9012	0	0.8270	0.0824	75.97
NHC 127	0.8538	0	0.7740	0.0935	41.58
NHC 128	0.7935	0	0.7385	0.0693	58.52
NHC 129	0.7476	0	0.6979	0.0664	60.74
NHC 130	0.7006	0	0.6636	0.0528	29.77
NHC 131	0.6492	0	0.6056	0.0673	58.69
NHC 132	0.5817	0	0.5501	0.0544	30.80
5-1	0.9503	0	0.8335	0.1230	136.03
5-2	0.9005	0	0.7968	0.1151	116.69
5-3	0.8495	0	0.6800	0.1996	480.30
5-4	0.7931	0	0.7633	0.0375	39.70

6. DISCUSSION

Direct comparisons between the data acquired in this study and the results obtained by previous investigators are difficult to make because the *P–T–X* conditions of prime interest here have not previously been extensively investigated (cf. Table 1). Figure 4 summarizes the phase relations determined in our experiments and compares them with the results of Bowers and Helgeson (1983). The two are significantly different. The model of Bowers and Helgeson (1983) places the vapor corner of the three-phase field at relatively low H_2O contents—~5 mol percent—in contrast with our experiments, which suggest a location above 63 mol percent. At the pressure and temperature of our experiments, the Bowers and Helgeson (1983) model was based largely on the data of Takenouchi and Kennedy (1965) and Gehrig (1980). The experiments of Gehrig (1980) were performed with samples containing 6, 10, and 20 weight percent NaCl at temperatures to 550°C and pressures to 3000 bar, and those of Takenouchi and Kennedy (1965) were performed at 6 and 20 weight percent NaCl at temperatures to 450°C and pressures to 1400 bar. This is equivalent to approximately 1.9, 3.3, and 7.2 mol percent NaCl on the H_2O-NaCl join and 4.6, 7.7, and 15.8 mol percent NaCl on the CO_2-NaCl join. Comparison of these compositions with the phase equilibria for the ternary system suggested by our experiments shows that they lie primarily in, or close to, the vapor field. Thus the experiments of Takenouchi and Kennedy (1965) and Gehrig (1980) place only weak constraints on the location of the three-phase field, which may explain why the model of Bowers and Helgeson (1983) predicts anomalously low H_2O contents for the vapor corner of the three-phase field.

Two other models for the H_2O-CO_2-NaCl system, those of Naumov et al. (1974) and Duan et al. (1995), are also based on limited datasets. The model of Naumov et al. (1974) was developed from the experimental data of Takenouchi and Kennedy (1964) and from fluid inclusions with mole fractions of NaCl up to 0.29, but mole fractions of CO_2 only up to 0.69. The model of Duan et al. (1995) is based on the ternary experiments of Takenouchi and Kennedy (1964), Gehrig (1980), Kotel'nikov and Kotel'nikova (1990), Frantz et al. (1992), and Joyce and Holloway (1993). The data of Kotel'nikov and Kotel'nikova (1991) were obtained from synthetic fluid inclusions in quartz at pressures higher than those of interest here (1000–2000 bar) and, within the ternary system, mole fractions of NaCl no higher than 0.13 at 500°C. While Kotel'nikov and Kotel'nikova (1991) noted the presence of halite in some of their samples, no attempt was made to delineate the three-phase field. Frantz et al. (1992) also acquired data from synthetic fluid inclusions in quartz at higher pressures (1000–3000 bar) than that of our experiments, and their 500°C, 1000 bar data were limited to mole fractions of NaCl no greater than 0.062. However, extrapolation of their data to lower pressures suggests lower solubilities of NaCl for intermediate H_2O-CO_2 compositions than obtained in our experiments. The reasons for this difference are unclear. Like Kotel'nikov and Kotel'nikova (1991), Frantz et al. (1992) found halite in some of their samples; however, they suggested that it formed during quenching. If so, phase-equilibrium data may be difficult to obtain by the synthetic fluid inclusion method. Joyce and Holloway (1993) performed fixed-H_2O activity experiments on vapor-brine assemblages at higher pressures and temperatures than those of interest here. Their results indicate the presence of a three-phase field with a vapor corner at relatively high H_2O contents.

The morphology of the H_2O-CO_2-NaCl phase diagram delineated in this paper has important implications for the thermodynamics of metamorphic fluids during decarbonation reactions. Because the amount of NaCl in the halite-saturated vapor decreases with increasing X_{CO_2} (Fig. 1), the activity of NaCl in most NaCl-bearing fluids must increase during decarbonation. Even if the NaCl content of the fluid is relatively small, the activity of NaCl may increase substantially during addition of CO_2 to the fluid. This is because the activity of NaCl along the saturation surface must be fixed. Thus, halite can precipitate from even relatively NaCl-poor fluids at elevated X_{CO_2} if decarbonation proceeds far enough.

The results presented in this paper show that the fixed-H_2O activity technique works well for H_2O-CO_2-NaCl fluids and that NaCl solubility experiments can be used to locate the positions of important phase boundaries in the H_2O-CO_2-NaCl system. Our data show that the vapor corner of the three-phase field occurs at a relatively high a_{H_2O}, they provide a major contribution to the accuracy of *a–X* models, and they provide a

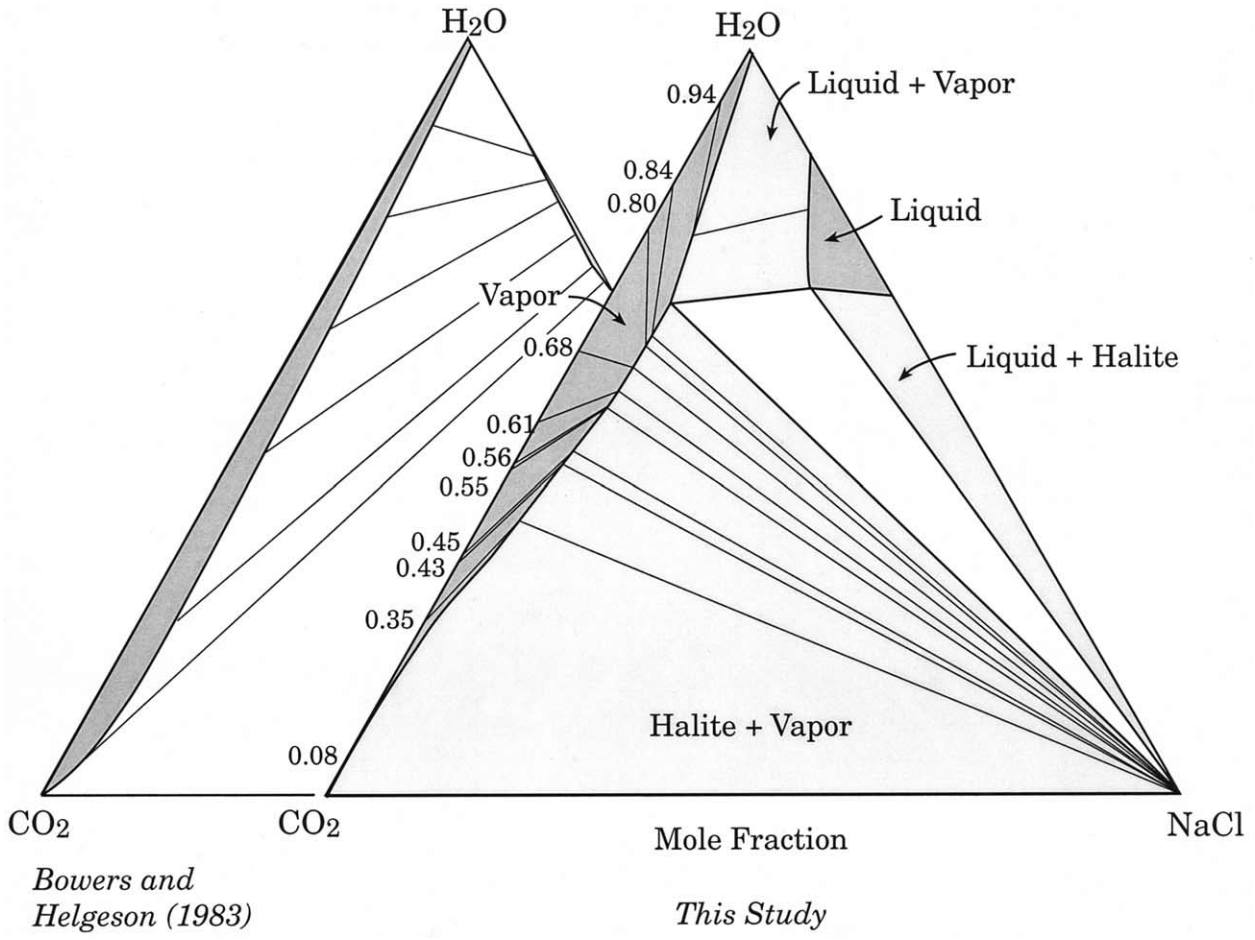

Fig. 4. Summary of the determined phase equilibria and isoactivity tie-lines for the H_2O-CO_2-NaCl system at 500°C, 500 bar. The isoactivity lines in the vapor field are fixed at the H_2O–CO_2 side and at the vapor-saturation curve. They need not be straight lines within the vapor field.

basis from which experiments at both higher pressures and temperatures can be planned.

Acknowledgments—We thank Leonya Aranovich, John Ferry, and an anonymous reviewer for their comments and insightful critiques of an earlier version of this paper. Funding for the research was primarily provided by the National Science Foundation under grant number EAR-0106990. Additional funding for the research was provided by (1) the Division of Engineering and Geosciences, Office of Basic Energy Sciences, U.S. Department of Energy, under Contract DE-AC05-96OR22464 with Oak Ridge National Laboratory, managed by UT-Battelle Corporation, and by (2) the U. S. Department of Energy, Environmental Management Science Program (TTP OR17-SP22), under contract number DE-AC05-96OR22464 with Oak Ridge National Laboratory, managed by UT-Battelle Corporation.

Associate editor: D. A. Sverjensky

REFERENCES

Ackerman F. J. and Koskinas G. J. (1972) Permeation of hydrogen and deuterium through palladium-silver alloys. *J. Chem. Eng. Data* **17,** 51–55.

Anderko A. and Pitzer K. S. (1993) Equation-of-state representation of phase equilibria and volumetric properties of the system NaCl-H_2O above 573 K. *Geochim. Cosmochim. Acta* **57,** 1657–1680.

Anovitz L. M., Blencoe J. G., Joyce D. B., and Horita J. (1998) Precise measurement of the activity-composition relations of H_2O-N_2 and H_2O-CO_2 fluids at 500°C, 500 bar. *Geochim. Cosmochim. Acta* **62,** 815–829.

Anovitz L. M., Labotka T. C., and Blencoe J. G. (2002) Experimental determination of phase equilibria in the system H_2O-CO_2-NaCl at 0.5 kb from 500 to 700°C. *Geol. Soc. Am. Abstr. Prog.* **34,** 363.

Aranovich L. Y. and Newton R. C. (1996) H_2O activity in concentrated NaCl solutions at high pressures and temperatures measured by the brucite-periclase equilibrium. *Contribs. Mineral Petrol.* **125,** 200–212.

Aranovich L. Y. and Newton R. C. (1999) Experimental determination of CO_2-H_2O activity-composition relations at 600–1000°C and 6–14 kbar by reversed decarbonation and dehydration reactions. *Am. Mineral.* **84,** 1319–1332.

Bigeleisen J., Perlman M. L., and Prosser H. C. (1952) Conversion of hydrogenic materials to hydrogen for isotopic analysis. *Anal. Chem.* **24,** 1356–1357.

Bischoff J. L. (1991) Densities of liquids and vapors in boiling NaCl-H_2O solutions: A *PV*Tx summary from 300 to 500°C. *Am. J. Sci.* **291,** 309–338.

Bischoff J. L. and Pitzer K. S. (1989) Liquid-vapor relations for the system NaCl-H_2O: Summary of the *P-T*-x surface from 300° to 500°C. *Am. J. Sci.* **289,** 217–248.

Blencoe J. G., Seitz J. C., and Anovitz T. M. (1999) The CO_2-H_2O system II. Calculated thermodynamic mixing properties for 400°C, 0–400 MPa. *Geochim. Cosmochim. Acta* **63,** 2293–2408.

Bodnar R. J. (1994) Synthetic fluid inclusions XII. Experimental determination of the halite liquidus and isochores for a 40 wt % H_2O-NaCl solution. *Geochim. Cosmochim. Acta* **58,** 1053–1063.

Bowers T. S. and Helgeson H. C. (1983) Calculation of the thermodynamic and geochemical consequences of nonideal mixing in the system H_2O-CO_2-NaCl on phase relations in geologic systems: Equation of state for H_2O-CO_2-NaCl fluids at high pressures and temperatures. *Geochim. Cosmochim. Acta* **47,** 1247–1275.

Brown E. and Lamb W. M. (1989) *P-V-T* properties of fluids in the system $H_2O \pm CO_2 \pm$ NaCl: New graphical presentations and implications for fluid inclusion studies. *Geochim. Cosmochim. Acta* **53,** 1209–1221.

Chou I.-M. (1987) Oxygen buffer and hydrogen sensor techniques at elevated pressures and temperatures. In *Hydrothermal Experimental Techniques,* Chap. 3, pp. 61–99. Wiley-Interscience.

Copeland C. S., Silverman J., and Benson S. W. (1953) The system NaCl-H_2O at supercritical temperatures and pressures. *J. Chem. Phys.* **21,** 12–16.

Darimont A. (1987) Compositon d'un fluide et trace de l'isochore dans le systeme H_2O-NaCl-CO_2. *Ann Soc. Géol. Belg.* **110,** 385–388.

Drummond S. E Jr. (1981) Boiling and mixing of hydrothermal fluids: Chemical effects on mineral precipitation. Ph.D. thesis Pennsylvania State University.

Duan Z., Moller N., and Weare J. H. (1995) Equation of state for the NaCl-H_2O-CO_2 system: prediction of phase equilibria and volumetric properties. *Geochim. Cosmochim. Acta* **59,** 2869–2882.

Ellis A. J. and Golding R. M. (1963) The solubility of carbon dioxide above 100°C in water and in sodium chloride solutions. *Am. J. Sci.* **261,** 47–60.

Frantz J. D., Popp R. K., and Hoering T. C. (1992) The compositional limits of fluid immiscibility in the system H_2O-NaCl-CO_2 as determined with the use of synthetic fluid inclusions in conjunction with mass spectrometry. *Chem. Geol.* **98,** 237–255.

Gehrig M. (1980) Phasengleichgewichte und PVT-Daten ternärer Mischungen aus Wasser, Kohlendioxid und Natriumchorid bis 3 kbar und 550°C. University of Karlsruhe, doctorate dissertation, Hochschul Verlag, Freiburg.

Grjotheim K., Heggelund Krohn C., and Motzfeldt K. (1962) On the solubility of CO_2 in molten halides. *Acta Chem. Scand.* **16,** 689–694.

Gunter W. E., Myers J. Girsperger G. (1987) Hydrogen: metal membranes. In *Hydrothermal Experimental Techniques,* Chap. 4, pp. 100–120. Wiley-Interscience.

Hendel E. M. and Hollister L. S. (1981) An empirical solvus for CO_2-H_2O-2.6 wt% salt. *Geochim. Cosmochim. Acta* **45,** 225–228.

Holleck G. L. (1970) Diffusion and solubility of hydrogen in palladium and palladium-silver alloys. *J. Phys. Chem.* **74,** 503–511.

Huebner J. S. (1971) Buffering techniques for hydrostatic systems at elevated pressures. *In Research Techniques for High Pressure and High Temperature* (ed. Ulmer G. C.), pp. 123–177. Springer-Verlag.

Jacobs G. K. and Kerrick D. M. (1981) Devolatilization equilibria in H_2O-CO_2 and H_2O-CO_2-NaCl fluids: An experimental and thermodynamic evaluation at elevated pressures and temperatures. *Am. Mineral.* **66,** 1135–1153.

Johnson E. L. (1992) An assessment of the accuracy of isochore location techniques for H_2O-CO_2-NaCl fluids at granulite facies pressure-temperature conditions. In *Current research on fluid inclusions; PACROFI III; papers presented at the Third biennial pan-American conference on Fluid inclusions. Geochim. Cosmochim. Acta* (eds. R. J. Bodnar and E. T. C. Spooner), pp. 295–302. Oxford, International, Pergamon.

Johnson E. L. and Jenkins D. M. (1991) Synthetic H_2O-CO_2 fluid inclusions in spontaneously nucleated forsterite, enstatite, and diopside hosts; the method and applications. *Geochim. Cosmochim. Acta* **55,** 1031–1040.

Joyce D. B. and Blencoe J. G. (1994) Excess molar Gibbs free energies for $\{xH_2O + (1-x)CO_2\}$ at temperatures from 673 K to 973 K at the pressure 50 MPa. *J. Chem. Therm.* **26,** 765–777.

Joyce D. B. and Holloway J. R. (1993) An experimental determination of the thermodynamic properties of H_2O-CO_2-NaCl fluids at high pressures and temperatures. *Geochim. Cosmochim. Acta* **57,** 733–746.

Keevil N. B. (1942) Vapor pressure of aqueous solutions at high temperatures. *Am. Chem. Soc. J.* **64,** 841–850.

Knight C. L. and Bodnar R. J. (1989) Synthetic fluid inclusions IX. Critical *PVTX* properties of the system H_2O-NaCl solutions. *Geochim. Cosmochim. Acta* **53,** 3–8.

Kotel'nikov A. R. and Kotel'nikova Z. A. (1990) Eksperimental'noye izucheniye fazovogo sostoyaniya sistemy H_2O-CO_2-NaCl metodom sinteticheskikh flyuidnykh vklyucheniy v kvartse. *Geokhim.* **1990 (*4*),** 526–537.

Kotel'nikova Z. A. and Kotel'nikov A. R. (1997) Modelirovaniye flyuidnogo rezhima retrogradnogo etapa metamorfizma na osnove eksperimental'nykh dannykh po fazovym ravnovesiyam v sisteme H_2O-CO_2-NaCl. *Petrolog* **5,** 73–80.

Levelt-Sengers J. M. H. and Gallagher J. S. (1990) Generalized corresponding states and high-temperature aqueous solutions. *J. Phys. Chem.* **94,** 7913–7922.

Lvov S. N. and Wood R. H. (1990) Equation of state of aqueous NaCl solutions over a wide range of temperatures, pressures, and concentrations. *Fluid Phase Equ.* **60,** 273–287.

Malinin S. D. and Kurovskaya N. A. (1975) The solubility of CO_2 in chloride solutions at elevated temperatures and CO_2 pressures. *Geochem. Int.* **12,** 199–201.

Malinin S. D. and Savelyeva N. I. (1972) The solubility of CO_2 in NaCl and $CaCl_2$ solutions at 25, 50, and 75°C under elevated CO_2 pressures. *Geochem. Int.* **9,** 410–417.

Morey G. W. (1957) The solubility of solids in gases. *Econ. Geol.* **52,** 225–251.

Naumov B., Khakimov A. K., and Khodakovskiy I. L. (1974) Solubility of carbon dioxide in concentrated chloride solutions at high temperatures and pressures. *Geochem. Int.* **11,** 31–41.

Ölander A. and Liander H. (1950) The phase diagram of sodium chloride and steam above the critical point. *Acta Chem. Scand.* **4,** 1437–1445.

Pabalan R. T. and Pitzer K. S. (1990) Models for aqueous electrolyte mixtures for system extending from dilute solutions to fused salts. *Am. Chem. Soc. Symp. Ser.* **416,** 44–57.

Pitzer K. S. (1984) Ionic fluids. *J. Phys. Chem.* **88,** 2689–2697.

Pitzer K. S. and Pabalan R. T. (1986) Thermodynamics of NaCl in steam. *Geochim. Cosmochim. Acta* **50,** 1445–1454.

Pitzer K. S. and Simonson J. M. (1986) Thermodynamics of multicomponent, miscible, ionic systems: Theory and equations. *J. Phys. Chem.* **90,** 3005–3009.

Plyusnina L. P. (1990) Eksperimental'noye issledovaniye ustoychivosti epidota v khloridno-karbonatnykh rastvorakh. *Geokhim.* **1990 (*1*),** 26–35.

Popp R. K. Frantz J. D. (1989) Fluid immiscibility in the system H2O-NaCl-CO_2 as determined from synthetic fluid inclusions. *Ann. Rep. Dir. Geophys. Lab. 1989–1990,* 43–48.

Rubin L. R. (1966) Permeation of deuterium and hydrogen through palladium and 75 palladium—25 silver at elevated temperatures and pressures. *Engel. Ind. Tech. Bull.* **7,** 55–62.

Schmidt C. (1997) Experimental study of the PVTX properties in part of the ternary system H_2O–NaCl-CO_2. Ph. D. thesis. Virginia Polytechnic Institute and State University, 49 p.

Seitz J. C. and Blencoe J. G. (1999) The H_2O-CO_2 system. I. Experimental determination of volumetric properties at 400°C and 10–100 Mpa. *Geochim. Cosmochim. Acta* **63,** 1559–1569.

Shaw H. R. (1963) Hydrogen-water vapor mixtures: control of hydrothermal atmospheres by hydrogen osmosis. *Science* **139,** 1220–1222.

Shaw H. R. (1967) Hydrogen osmosis in hydrothermal experiments. *In Researches in Geochemistry* (ed. Abelson P. H.) 2, pp. 521–541, Wiley.

Shmulovich K. I. and Plyanusova N. V. (1993) Phase equilibria in ternary systems formed by H_2O and CO_2 with $CaCl_2$ or NaCl at high *P* and T. *Geochem. Int.* **30,** 53–71.

Shmulovich K. I. and Graham C. M. (1996) Melting of albite and dehydration of brucite in H_2O-NaCl fluids to 9 kbar and 700–900°C: implications for partial melting and water activities during high pressure metamorphism. *Contrib. Mineral. Petrol.* **124,** 370–382.

Shmulovich K. I. and Graham C. M. (1999) An experimental study of phase equilibria in the system H_2O-CO_2-NaCl at 800°C and 9 kbar. *Contrib. Mineral. Petrol.* **136,** 247–257.

Sourirajan S. and Kennedy G. C. (1962) The system H_2O-NaCl at elevated temperatures and pressures. *Am. J. Sci.* **260,** 115–141.

Sterner S. M., Chou I-M., Downs R. T., and Pitzer K. S. (1992) Phase relations in the system NaCl-KCl-H_2O: V. Thermodynamic-*PTx* analysis of solid-liquid equilibria at high temperatures and pressures. *Geochim. Cosmochim. Acta* **56,** 2295–2309.

Sterner S. M, Kerrick D. M, Bodnar R. J. (1984) Experimental determination of unmixing in H_2O-CO_2-NaCl fluids at 500 degrees C and 1 Kb using synthetic fluid inclusions; metamorphic implications, The Geological Society of America, 97th annual meeting: Abstracts with Programs—Geological Society of America. Boulder, CO, United States, Geological Society of America (GSA), 668.

Takenouchi S. and Kennedy G. C. (1964) The solubility of carbon dioxide in NaCl solutions at high temperatures and pressures. *Am. J. Sci.* **263,** 445–454.

Tanger J. C. and Pitzer K. S. (1989) Thermodynamics of NaCl-H_2O: A new equation of state for the near-critical region and comparisons with other equations for adjoining regions. *Geochim. Cosmochim. Acta* **53,** 973–988.

Tödheide K. and Franck E. U. (1963) Die Zweiphasengebiet und die kritische Kurve im System Kohlendioxid—Wasser bis zu Drucken von 3,500 bar. *Zeitsch. Physikal. Chem. N. Folge* **37,** 387–401.

Yasunishi A. and Yoshida F. (1979) Solubility of carbon dioxide in aqueous electrolyte solutions. *J. Chem. Eng. Data* **24,** 11–14.